Laser-Assisted Reduction of Graphene Oxide for Flexible, Large-Area Optoelectronics

Emmanuel Kymakis, *Member, IEEE*, Constantinos Petridis, Thomas D. Anthopoulos, and Emmanuel Stratakis

(Invited Paper)

***Abstract*—This paper reviews recent work on the development and use of a low-temperature, laser-based method for the efficient reduction of graphene oxide (GO) films. The method utilizes a laser beam for the *in-situ* and nonthermal reduction of solution-processed GO layers onto arbitrary substrates. Compared to other reduction techniques, it is single-step, facile, and can be performed at room temperature in ambient atmosphere without affecting the integrity of the either the graphene lattice or the physical properties of the underling substrate. Using this method, conductive layers of reduced GO with a sheet resistance down to ∼700 Ω/sq, are obtained. This is much lower than sheet resistance values reported previously for GO layers reduced by chemical means. As a proof of concept, laser-reduced GO layers were successfully utilized as the transparent anode electrodes in flexible bulk-heterojunction OPVs and as the channel material in field-effect transistors. To the best of our knowledge, this is the only example of an *in-situ*, postfabrication method for the reduction of GO and its implementation in fully functional opto/electronic devices. The nonthermal nature of the method combined with its simplicity and scalability, makes it very attractive for the manufacturing of future generation large-volume graphene-based opto/electronics.**

***Index Terms*—Flexible electronics, graphene, graphene oxide (GO), organic photovoltaics (OPVs), transistors.**

I. Introduction

SOLUTION-processable semiconductors represent a fast emerging technology that promises to replace traditional inorganic semiconductors, such as silicon, in a number of established as well as novel electronic applications [1]. This is primarily due to their numerous advantages that include; compatibility with solution-based large-area processing and inexpensive flexible substrate materials, as well as control of their electrical, magnetic, and optical properties [2], [3].

Although the family of solution-processable semiconductors includes both organic as well as inorganic materials, the branch of electronics based on them is often called organic/plastic electronics [4]. Flexible electronics [5] have been a growing part of research and development in organic electronics due to their expanding applications, including touch screens, optical displays, photovoltaics, lighting devices, and sensors [6]. This technology is based on the controlled deposition and/or printing of different solution-processed layers that form the various device components, onto mechanically flexible substrates [5]. A critical requirement for this technology is that the fabrication processes must be compatible with the nominally low-temperature plastic materials that are being considered for the substrates. In addition to the electrical and optical properties, the ideal solution-processable electronic material should be mechanically robust under extensive bending. Recent research has focused on the development of conductive and semiconductive flexible nanolayers based on composites of carbon nanotubes (CNTs) [7] and nanowire networks [8], [9]. Although such materials are suitable for low cost, large area flexible electronic applications, the nanometers-thick layers developed to date exhibit relatively high roughness. The latter characteristic limits the applicability of these technologies since it is often found to reduce the manufacturing yield of the respective devices.

Owing to its 2-D structure and the resulting unique electronic properties (ballistic charge transport, etc.), graphene has attracted significant interest for use in a host of opto/electronic applications [10], [11]. Indeed, solution-processed graphene derivatives were proved to be strong candidates for flexible electronic devices including transparent electrodes [12], field-effect transistors (FETs) [13], field emitters [14], electron acceptors [15], and buffer layers [16] in photovoltaic devices. As a result, much attention has been paid to the mass production of large-area graphene layers. Production techniques reported to date include mechanical [17] and chemical [18] exfoliation as well as thermal and plasma [19], [20] enhanced chemical vapor deposition. Another very promising and cost effective method is the reduction of solution processable graphene oxide (GO) [21]. The latter can be easily produced by exfoliation in aqueous solution of inexpensive graphite oxide to form sheets comprising single or few layers of carbon atoms decorated with oxygenated species. Among the numerous advantages of GO, many of which not provided by any other production technique, is that it is highly hydrophilic, thus it can form stable aqueous

Manuscript received May 23, 2013; revised June 28, 2013; accepted July 8, 2013. Date of publication August 1, 2013; date of current version August 29, 2013.

E. Kymakis is with the Center of Materials Technology and Photonics and the Department of Electrical Engineering, Technical Educational Institute of Crete, 71004 Heraklion, Greece (e-mail: kymakis@staff.teicrete.gr).

C. Petridis is with the Center of Materials Technology and Photonics, Technical Educational Institute of Crete, 71004 Heraklion, Greece and also with the Department of Electronic Engineering, Technical Educational Institute of Crete, 73135 Chania, Greece (e-mail: c.petridis@chania.teicrete.gr).

T. D. Anthopoulos is with the Department of Physics and the Centre for Plastic Electronics, Imperial College London, London SW7 2 BW, U. K. (e-mail: thomas.anthopoulos@imperial.ac.uk).

E. Stratakis is with the Institute of Electronic Structure and Laser, Foundation for Research and Technology–Hellas, and also with the Department of Materials Science and Technology, University of Crete, 71003 Heraklion, Greece (e-mail: stratak@iesl.forth.gr).

Color versions of one or more of the figures in this paper are available online at http://ieeexplore.ieee.org.

Digital Object Identifier 10.1109/JSTQE.2013.2273414

colloids which in turn can facilitate the assembly of macroscopic structures and large-area devices using simple and inexpensive solution-based processing methods. On the other hand, the product of the reduction process, commonly referred to as reduced GO (r-GO), is of moderate electrical performance when compared to graphene, mainly due to the presence of oxygen-related defects in the graphene lattice. Therefore, the principal aim of each reduction technique is to yield a material as close in structure and physical properties to graphene as possible [22].

Reduction of GO is often achieved via chemical reaction with reducing agents and/or high temperature annealing under inert atmosphere [12], [23]. Such reduction processes, apart from the facts that are time-consuming and complex, are often not compatible with inexpensive flexible substrates, such as polyethylene terephthalate (PET), since the latter cannot withstand high temperatures ($>250\,^{\circ}$C) or corrosive chemical agents. One plastic-compatible method that has recently been used to fabricate flexible organic photovoltaic (OPV), relies on a physically transferred r-GO film as the transparent electrode [24]. However, in this case, the GO was initially spin coated on a SiO_2/Si substrate, therefore, an additional processing step the transfer to the PET electrode is required, resulting in high cost and complexity in the device fabrication [25]. Furthermore, there are issues concerning the efficiency of the transferring process in large areas. Therefore, a low cost, fast and compatible technique with flexible substrates is highly desirable. Most recently, several groups have demonstrated that GO solution can be reduced by photoirradiating process, such as UV-induced photocatalytic reduction [26], photothermal reduction using a pulsed Xenon flash [27] or selective laser reduction and patterning [28]. Among the advantages are that laser-irradiating processes do not rely on the use of chemicals or high temperatures; especially, shorten the reaction time from several hours to a few minutes [29].

In this paper, we review the latest results on the development and use of a novel, facile, *in-situ*, and fast GO reduction technique that is compatible with large-area plastic opto/electronics. The method does not require the use of any chemicals or high temperature annealing. The primary advantage of this technique lies in the ability for the *in-situ* controlled epidermal treatment without practically affecting the integrity of the underlying substrate. Furthermore, it can be applied as a postfabrication step without compromising any of its components. As a proof of concept, laser-reduced GO (LrGO) films were utilized as the transparent electrode in flexible OPVs [30] as well as for the *in-situ* treatment of solution-processed GO-based FETs where it is found to remarkably affect the electronic performance of the devices [31]. The combination of the unique characteristics associated with the proposed *in-situ* method suggest that it can be used for roll to roll processing of GO films for application in large-volume, plastic electronics.

II. Experimental Details

A. Preparation of GO Films

GO was prepared from purified natural graphite powder (Alfa Aesar) according to modified Hummers' method [32]. Specifically, graphite powder (0.5 g) was placed into a cold mixture of concentrated H_2SO_4 (40 mL, 98%) and $NaNO_3$ (0.375 g) under vigorous stirring for 1 h, in an ice bath. During this time, $KMnO_4$ (2.25 g) was added in portions and the ice bath was kept for 2 h more, in order to cool the mixture under 10 °C. The green–brown colored mixture remained for stirring for five days. On completion of the reaction, the brick colored mixture was mixed with an aqueous solution 5% H_2SO_4 (70 mL). The mixture was stirred for 1 h under heating at 98 °C and becomes gray–black colored. When the temperature was decreased at 60 °C, 30% H_2O_2 ($\sim$2 mL) was added and the mixture was stirred for 2 h at room temperature. In order to remove acidic ions, especially these of Mn, we used the following process. The mixture was centrifuged for 5 min at 4200 r/min and washed with $\sim$600 mL of an aqueous solution of 3% H_2SO_4 ($\sim$9 mL)/0.5% H_2O_2 ($\sim$1.5 mL), and then, was put in an ultrasonic vibration bath for 10 min (The ultrasonic vibration exfoliates the graphite oxide to GO sheets). The process was repeated for ten times. Then, the mixture washed and purified with 150 mL of aqueous solution 3% HCl ($\sim$1.5 mL) for three times. Afterwards, it is washed thoroughly with distilled water (1D) and acetone, in order to remove any acidic part remaining. Finally, the material was dried to obtain a loose brown powder which can be stored indefinitely [33]. For the preparation of the electrodes, flexible PET (Goodfellow) pieces (15 mm $\times$ 15 mm) with 90-μm thickness were used as substrates. PET substrates were cleaned by detergent followed by ethanol and Milli-Q water, and subsequently, treated by the O_2 plasma to provide a more hydrophilic surface. For the preparation of the thin films, 15-mg/ml GO solution in ethanol was spin coated at 1000 r/min onto the PET substrates. The initial volume of the GO solution was used as a mean to control the thickness of spin-coated GO films. Following the spin coating process, the GO films were dried at 70 °C inside a nitrogen filled glove box. For the experiments, a series of films were produced, while their thickness was measured using AFM images of steps defined at their edges. The sheet resistance was measured in a four electrode configuration and includes the contact resistance between the graphene film and thermally evaporated gold electrodes used to probe the films.

B. Pulsed Laser Reduction of GO Films

The pulsed laser reduction system consists of a Ti:Sapphire (Tsunami,Spectra-Physics) laser ($\lambda = 800$ nm) delivering 100 fs pulses at a repetition rate of 1 kHz. The laser beam was focused down to 170 μm onto the GO film using a 10-mm lens. For the experiments, the laser output power was varied in the range of 1.0–10 mW corresponding to fluences of 3.5–35 mJ/cm^2. GO films were mounted on a high-precision $X-Y$ translation stage normal to the incident laser beam. A mechanical shutter was synchronized to the stage motion to provide for a uniform exposure of the sample area to a constant number of pulses. In order to investigate the repetition rate effect on the reduction process, pulses from a femtosecond (fs) laser oscillator of 800 nm, 100-fs pulse duration, and 80-MHz repetition rate, were used. In order to investigate the effect of pulse duration, pulses from a KrF excimer laser of 248 nm, 30-ns pulse duration, and 10-Hz

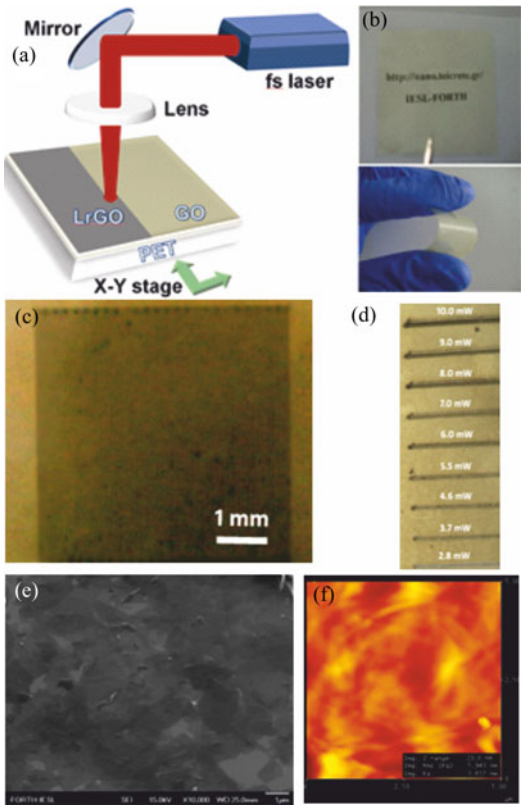

Fig. 1. (a) Irradiation scheme of the LrGO films preparation. (b) Typical photo of a flexible GO film. (c) Large processed area and (d) scan lines obtained upon irradiation with 100-fs pulses at different fluences indicating the gradual color change due to reduction. (e) SEM and (f) AFM images of LrGO films on PET. From [30]

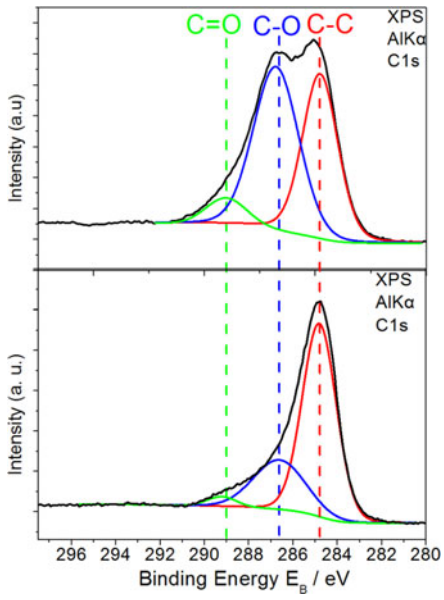

Fig. 2. (Top) XPS measurements of GO films and (bottom) LrGO films. The content of the carbon to oxygen bonds have been reduced from 61% to 16% indicating the removal of the majority of the oxygen groups [30].

repetition rate were used. In all cases the range of fluences used was the same.

III. Results and Discussions

A. *In-Situ Laser Reduction of Spin-Coated GO Films on PET*

Fig. 1(a) depicts the irradiation scheme used for the preparation of the LrGO films. The pulsed laser reduction system consists of a Ti:Sapphire (laser ($\lambda = 800$ nm) delivering 100 fs pulses at a repetition rate of 1 kHz. GO films were mounted on a high-precision $X-Y$ translation stage normal to the incident beam. The laser beam was focused down to 170 μm onto the GO film using a 10-mm lens. For the experiments, the laser output power was varied in the range of 1.0–10 mW corresponding to fluences of 3.5–35 mJ/cm^2.

During the reduction process, the as-spun GO layers on PET [see Fig. 1(b)] were irradiated by the fs laser beam that was translated onto the film area. It is observed that the yellowish color of the pristine film was gradually turned into black [see Fig. 1(c)], indicating that GO is rapidly reduced via the laser treatment in air without the use of any reducing agents [34]. By carefully tuning key laser parameters, the reduction degree of GO could be controlled in the irradiated region. For example, Fig. 1(d) depicts scans lines obtained upon increasing the irradiation power. As the level of the reduction process progresses, a gradual change in the coloration of the GO film from yellowish to dark brown, and finally, black was observed [35].

In order to check that only minor ablation has been occurred on the surface of the laser-treated GO films, SEM and AFM analysis performed. Fig. 1(e) and (f) shows the results of the SEM and AFM analysis confirming that the roughness of the irradiated area has not been affected by the laser treatment process. Some dark spots that were observed correspond to localized areas with lower ablation thresholds. These dark spots are suspected to be there due to thermal effects during the laser reduction process that deforms the GO/PET interface.

This significant reduction of the GO sheets is evidenced by XPS measurements, shown in Fig. 2. The C1s XPS spectrum of pristine GO exhibits three components that correspond to carbon atoms in different functional groups: the nonoxygenated ring C, the C in C–O bonds, and carboxylate carbon (C=O). Notably, the carbon content bonded to oxygen is reduced from 61% in the initial GO to 16% in LrGO indicating that the majority of oxygen groups were removed. It should be emphasized that such improvement can be achieved without any apparent damage in the mechanical properties and integrity of the PET substrate.

The major advantage of the proposed technique is that the combination of short laser pulses (fs) and the right repetition rate achieve very fast removal of the oxygen groups from the GO crystal without affecting thermally the graphene lattice and the deposition substrate. In order to support the effectiveness of the laser GO reduction on PET substrate, a theoretical simulation was carried out to provide an insight into the heat absorption and subsequent thermal effect on the temperature sensitive PET substrate [30]. In the particular case of fs laser irradiation of a nanometric film on a substrate under subablation conditions considered here, theoretical and experimental investigations indicate that the heating effects are much less pronounced

compared to the longer pulse irradiation due to the absence of electron–phonon coupling during the pulse.

A theoretical simulation was carried out to provide an insight into the heat absorption and subsequent thermal effect on the temperature sensitive PET substrate during the laser reduction process. To account for the maximum laser heating effect attained the simulation is performed in the case of irradiation with nanosecond laser pulses of the same fluence (17.5 mJ/cm^2) as that used for the fs reduction process. In this case, the dynamics of laser heating can be considered as a typical 3-D heat flow problem, which can be simulated by the solution of the heat conduction equation:

$$\rho C_p \frac{\partial T(r,t)}{\partial t} - \frac{\partial}{\partial x}\left(k\frac{\partial T(x,t)}{\partial x}\right) - \frac{\partial}{\partial y}\left(k\frac{\partial T(y,t)}{\partial y}\right) - \frac{\partial}{\partial z}\left(k\frac{\partial T(z,t)}{\partial z}\right) = S(x,y,z) \quad (1)$$

where ρ is the mass density, C_p is the specific heat, k is the thermal conductivity, and $S = \alpha I(x, y, z, t)$ is an internal heat source, with α to be the absorption coefficient. The x, y directions lie in the film plane, while z corresponds to the direction perpendicular to the film surface. The laser power density I has a Gaussian profile and can be considered to have a temporal and spatial part with an exponential decay and is written as:

$$I(x,y,z,t) = 0.94(1-R)I_o(x,y)\exp(-\alpha z) \times \exp\left[-4\ln 2\left(\frac{t}{t_p}\right)^2\right] \quad (2)$$

with

$$I_o(x,y) = \frac{J}{t_p}\exp\left[-\frac{x^2+y^2}{r_g^2}\right] \quad (3)$$

where R is the GO film reflectivity, J is the laser fluence, t_p is the pulse duration (i.e., full width at half maximum), and r_g is the radius of the Gaussian beam. A finite-element model (FEM) is used to calculate the temperature distribution around the spot center following irradiation of a 20.1-nm thin GO film on PET with 100 pulses of 20 ns at a fluence of 17.5 mJ/cm^2. Details of the FEM method can be found in [30].

Fig. 3 depicts the calculated temperature profile within a cross-sectional area of the GO/PET system and the corresponding temperature variation as a function of the depth from the GO film surface ($z = 0$). The highest attainable temperature is below 350 °C indicating that the laser heating might induce removal of oxygen functional groups, considering that the desorption of such groups from GO occurs around 200–230 °C [39]. During this reduction process, the PET substrate is slightly affected since, as shown in Fig. 3, a ~3-μm layer, corresponding to ~3.5% of its total thickness, is estimated to exceed its melting point.

In the particular case of fs laser irradiation of a nanometric film on a substrate under subablation conditions considered here, theoretical and experimental investigations indicate that the heating effects are much less pronounced compared to the longer pulse irradiation due to the absence of electron–phonon coupling during the pulse; under such conditions, nonthermal excitation effects become dominant [40]. Therefore, it is expected that the maximum attainable temperatures will be much lower than those calculated in Fig. 6 for the extreme case of nanosecond irradiation. This in turn supports our experimental evidence for nonthermal reduction of GO achieved upon irradiation with fs pulses. It should be noted here that it is difficult to perform simulations for the fs case, considering that some of the constants required for the calculation, i.e, electron and lattice specific heats, electron relaxation time, and electron–phonon coupling factor are not yet reported in the literature.

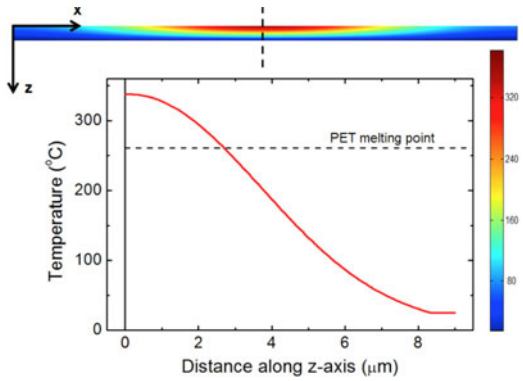

Fig. 3. Thermal modeling results: (top) cross-sectional contour plot showing the temperature distribution within a 320 μm × 9 μm area of the GO/PET system; (bottom) temperature gradient along z-axis (the surface of the GO film corresponds to $z = 0$). The dashed line indicates the melting temperature of PET. From [30]

B. LrGO Films as Transparent Electrodes in OPVs

Graphene-based materials are very promising candidates as transparent conductive electrodes in photovoltaics due to its high electrical conductivity and optical transmittance (T_R) [41]. In our technique, either of these properties can be individually tuned to the optimum value by changing the LrGO electrode thickness and the respective degree of reduction. Indeed, by carefully selecting key laser parameters, the reduction degree of GO could be readily controlled. Fig. 4(a) presents the dependence of the LrGO sheet resistance ($R_{\rm SH}$) as a function of the laser power used. It can be noticed that the conductivity of the LrGO films has been increased by two orders of magnitude with a small increase of the laser power. When the incident power exceeds 5.5 mW, the GO layers were partly ablated. Furthermore, for constant incident power, the film resistivity decreases upon increasing the average number of pulses per spot, N, until saturation is reached for high pulse numbers [see Fig. 4(b)]. It is concluded that there is an optimum combination of the laser energy and the number of laser pulses that can lead to at least three orders of magnitude reduction of sheet resistance.

In order to demonstrate the capabilities of the flexible LrGO films as transparent electrodes, $R_{\rm SH}$ and T_R were measured as a function of various film thicknesses. As was expected both of the measured quantities reduce with the increase of the films thickness [42].

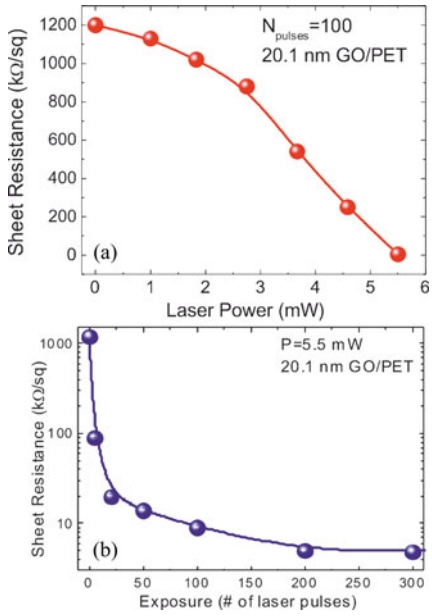

Fig. 4. (a) Dependence of LrGO films on fs laser output power. (b) Saturation effect in LrGO films with the number of laser pulses. From [30].

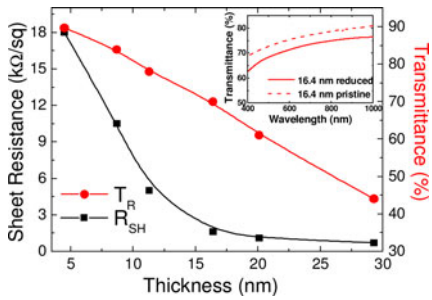

Fig. 5. (a) Transmittance at 550 nm and sheet resistance of the LrGO films on PET substrates as a function of their film thickness. The inset shows the UV–Vis transmittance spectra of the LrGO films on PET. From [30].

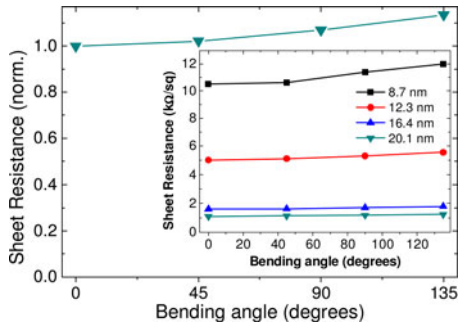

Fig. 6. Sheet Resistance (normalized to the unbending sheet resistance) for various bending angles and thicknesses. From [30]

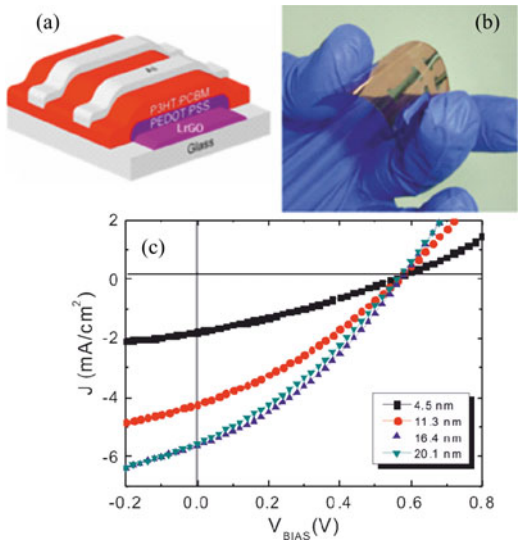

Fig. 7. (a) Schematic and (b) picture of the flexible PET/r-GO/PEDOT:PSS/P3HT:PCBM/Al photovoltaic devices fabricated; (c) illuminated current–voltage (*J–V*) curves of the solar cells with various LrGO film thicknesses. From [30]

Fig. 5 shows the $R_{\rm SH}$ and T_R at $\lambda = 550$ nm of LrGO films of different thicknesses. It is clear that both $(R_{\rm SH})$ and (T_R) decreased upon increasing the GO layer thickness. The obtained lowest $R_{\rm SH}$ is 0.7 kΩ/sq for the 20.1-nm thick LrGO film whose transmittance is 44%. The highest optical transparency of 88% was obtained for the 4.5-nm thick LrGO, but the sheet resistance is 18 kΩ/sq. The flexible electronics technology requires electrodes exhibiting high transparency and conductivity complemented by bendability [43]. Until recently, the OPV devices with bulk heterojunction (BHJ)-based active regions use transparent electrode made by indium tin oxide (ITO). However, the use of such metal oxides is problematic for various reasons: limited indium supply source, susceptibility to ion diffusion into polymer layers, brittle nature of metal oxide. On the top of this mechanical stress measurements using ITO show that this element can be easily fractured, and therefore, do not meet the flexible electronics technology standards. Particularly a substantial increase of the sheet resistance of ITO films has been demonstrated for bending angles higher than 45° [44]. Furthermore, the electrical characteristics of the conventional ITO films are degraded by at least three orders of magnitude after bending [45] (at a bending angle around 50–60°).

Fig. 6 depicts the averaged sheet resistance of the LrGO films with various thicknesses, normalized with the $R_{\rm SH}$ before bending, under different bending angles which are defined as the angles of intersections drawn from the two bent ends. It is observed that the electrical characteristics of the flexible LrGO films show no significant dependence on the bending angle. The inset shows the $R_{\rm SH}$ of the same films as a function of the bending angle. The change in $R_{\rm SH}$ becomes appreciable after the angle of 90°, while the overall change is less than 13% up to 135°. This implies that no appreciable cracks occur in the film during bending. The low resistance, high bending tolerance, and high absorption characteristics of the fabricated LrGO films are attractive features for these films to be incorporated into flexible electronic devices such as photovoltaics. For this purpose, the LrGO films were used as hole electrodes in flexible P3HT:PCBM photovoltaic devices. Fig. 7 presents the illuminated *J–V* characteristics of the OPV devices with LrGO thickness of 4.6, 11.3, 16.4, and 20.1 nm. The $V_{\rm OC}$ is constant at 0.57 V, while a variation is only observed for the device with

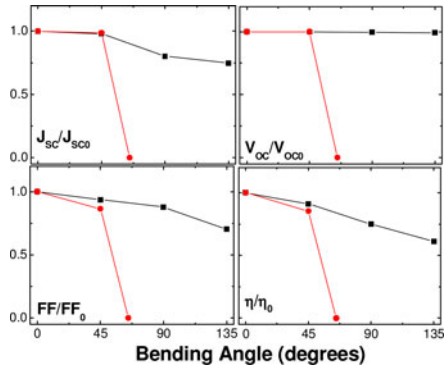

Fig. 8. Evolution of photovoltaic parameters of LrGO (squares) and ITO (circles) based OPV devices under bending in different angles. From [30]

the lowest LrGO thickness. This behavior is consistent, since $V_{\rm OC}$ is mainly governed by the energy levels offset between the highest occupied molecular orbital of P3HT and lowest unoccupied molecular orbital of PCBM. Both photocurrent and fill factor increase with increasing LrGO thickness, due to the reduction of the sheet resistance. The optimum thickness is about 16.4 nm, where a $J_{\rm SC}$ of 5.62 mA/cm^2, a $V_{\rm OC}$ of 0.57 V, a FF of 0.34, and an overall efficiency of 1.1% were obtained. This value is the highest observed so far, for flexible OPVs with r-GO film, indicating the effectiveness of the laser ablation reduction method [30].

In the case of GO reduction by thermal annealing in Ar/H_2 at 1000 °C, the best photovoltaic performance ($n = 0.78\%$) was achieved with a 16-nm thick LrGO film having $R_{\rm SH}$ of 3.2 kΩ/sq, and T_R of 65%. In our approach, where the reduction takes place by laser ablation, an efficiency enhancement by 41% is obtained with a 16.4-nm thick film having $R_{\rm SH}$ of 1.6 kΩ/sq, and T_R of 70%. Therefore, it is evident that the higher conductivity of the LrGO film is responsible for the higher efficiency, indicating the superiority of the laser ablation method, compared with the chemical one. Furthermore, the reduction process takes place *in situ* on the flexible spin-coated GO film, which is not the case in all other relevant work. The effect of mechanical property of LrGO films on the electrical properties of OPV devices was studied by monitoring the performance after applying tensile stress on the devices. Fig. 8 presents the results of the experiment monitoring the photovoltaic performance of flexible OPVs as a function of the bending angle. As it can be seen, the photovoltaic characteristics are slightly degraded upon bending, and are still functional even for bending angles up to 135°. In contrast, the traditional ITO-based OPV devices operate only for bending up to 45°, and fail completely at 65°. For the LrGO devices, as the bending angle increases, both the $J_{\rm SC}$ and FF decay, while $V_{\rm OC}$ remains constant.

This decay can be directly related to the decreased $R_{\rm SH}$ during bending, as shown in Fig. 8. Since the FF parameter highly depends on the LrGO electrode properties, the dependence of FF on the bending angle clearly demonstrates the superiority of the LrGO electrodes over the ITO electrodes in terms of flexibility.

C. Postfabrication Reduction of GO FETs

The proposed laser reduction GO technique has applied for the *in-situ* enhancement of the transport properties of prefabricated GO-based FETs [31]. Bottom-gate, bottom contact transistors structures were fabricated using heavily doped p-type Si wafers acting as a common back-gate electrode and a 200-nm thermally grown SiO_2 layer as the dielectric. Using conventional photolithography, the gold source–drain (S–D) electrodes were defined with channel lengths and widths in the range 1–40 μm and 1–20 mm, respectively. A 10-nm layer of titanium was used as an adhesion layer for the gold on SiO_2. The finished electrodes were 100-nm thick. The GO flakes were deposited by dip-coating at room temperature directly onto 1.5 cm × 1.5 cm size substrates containing few hundreds of prepatterned S–D electrode pairs. The as-prepared devices were then used directly without any thermal pretreatment. For the laser illumination experiments the devices were placed into a vacuum chamber, maintained at 10^{-2} mbar, and were illuminated by a KrF excimer laser (pulse width 20 ns, 243 nm, 1 Hz repetition rate) beam. For the uniform illumination of the whole sample, a top-flat beam profile of 20 mm × 10 mm was obtained using a beam homogenizer. To ensure that the laser treatment is performed into an inert atmosphere, a constant He or N_2 pressure of 100 Torr was maintained during the process through a precision microvalve system. Different combinations of laser fluences (F) and number of pulses (N), were tried in an effort to study the effect of this parameter in the efficiency of the proposed laser-reduction process. Initial experiments show that the threshold fluence for reduction, defined, as the lowest F required improving sample's conductivity after single pulse exposure, lied in the range of 10–15 mJ/cm^2. Such F values were close to those predicted theoretically for the removal of oxygen groups from the GO lattice [40]. In a typical experiment, the sample was irradiated with $N = 10$, 20, 30, 40, 50, 60, 120, 600, and 1200 pulses, respectively, using a constant F. By carefully tuning the laser parameters, the degree of reduction of GO could be readily controlled. In particular, the conductivity of GO FETs can be increased by more than two orders of magnitude with a gradual increase of the laser energy. Fig. 9(a) shows the current level ($V_{\rm DS} = 5$ V) measured for a typical GO FET upon laser treatment with 600 pulses at different fluences.

It is evident that the reduction efficiency is dependent on the laser energy used and a threshold fluence is required for the initiation of the process. When the incident F exceeds 80 mJ/cm^2, degradation or even damage of the GO FETs was observed, possibly due to partial ablation of the GO layers. Besides this, for constant incident F, the channel resistivity decreases upon increasing N until saturation is reached for high pulse numbers. It is evident that a more than three orders of magnitude decrease in channel resistance can be realized via proper selection of F and N. Fig. 9(b) shows a representative series of output curves curves ($V_G = -20 \sim 20$ V) of a GO FET subjected to irradiation with different N at $F = 80$ mJ/cm^2. It can be seen that by increasing N, the conductivity of the GO channel progressively improves by more than three orders of magnitude. Notably, the channel conductivity appears to saturate after approximately

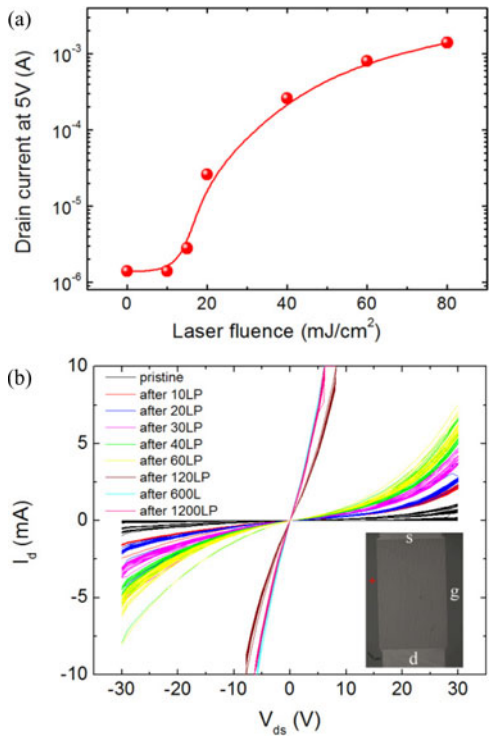

Fig. 9. (a) GO transistor currents levels measured at an applied bias of 5 V after the laser treatment at various fluences using 600 pulses; (b) Output characteristics of a pristine and *in-situ* laser processed r-GO FET treated at different pulse numbers. From [31].

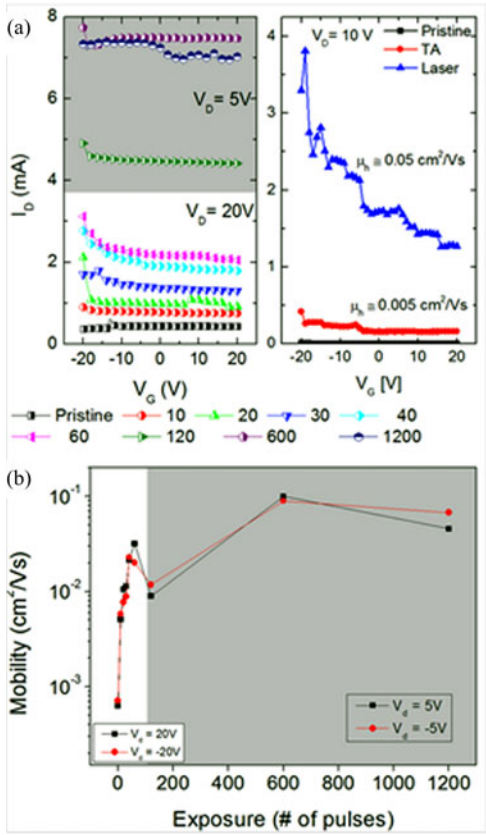

Fig. 10. (a) (Left) Corresponding transfer characteristics of r-GO FET treated at different pulse numbers under positive gate bias; (right) transfer characteristics of an r-GO FET in its pristine, thermally annealed (TA) and laser treated states, respectively. The respective hole mobilites are also indicated. (b) Impact of different laser pulse numbers on the device mobilities. From [31].

120 pulses, i.e., 2 min, most likely suggesting that the vast majority of oxygen groups have been removed from the GO lattice. The corresponding transfer characteristics of the pristine and the laser-treated GO FET under positive gate bias are displayed in Fig. 10 (a)-left part. A clear ascending trend in channel current (I_D) suggests the efficiency of increasing exposure times of the laser treatment. Fig. 10(b) displays the impact of different laser pulse numbers on the device mobilities.

It can be clearly seen that when increasing the laser pulses, the mobility has been significantly improved (from 6×10^{-4} cm^2/Vs to $\sim 1 \times 10^{-1}$ cm^2/Vs). Furthermore, as presented in Fig. 10 (a)-right part, the laser reduction process was found to be more efficient compared to thermal annealing (TA) at 200 °C in N_2. Indeed, the current levels and mobility obtained for a GO FET subjected to TA were lower by almost one order of magnitude than those measured on the same device subjected to the laser reduction after the TA treatment. Overall, the mobility improvement attained by the laser is comparable or even higher than the optimum ones reported using TA at 250 °C and flash reduction methods, respectively.

The various oxygen groups on the GO lattice are considered as defects and degrade the electrical characteristics of the FETs. The measured enhancement of the laser treated FETs mobilities is due to the elimination of these defects. In order to further investigate this hypothesis, the GO samples structural characteristics were examined by recording the micro-Raman spectrum of the illuminated area. Raman spectra were obtained using a micro-Raman spectrometer (NICOLET ALMEGA XR) with a 473-nm laser as the excitation source using low power in order not to damage the sample. The results are presented in Fig. 11.

All spectra feature the characteristic broad peaks at 1354, 1597, and 2695 cm^{-1}, corresponding to D, G, and 2-D bands of the GO lattice, respectively, as the pulse number increases both D and narrower [see Fig. 11(c)], while their intensities become progressively lower. Besides this, no appreciable band shift is observed. The peak intensities lowering can be attributed either to oxidative burning, which removes layers from the GO sheet [44] and/or to the reduction of interlayer spacing due to removal of the water and oxygen functional groups among GO sheets [45]. Furthermore, G and D peaks narrowing suggest the reestablishment of sp^2 carbons as well as a decrease in the structural defects within the basal planes of the laser treated GO [46], [47]. The overall changes in the G and D bands indicate a transition from an amorphous state to a more crystalline carbon state. Finally, the D over G peak intensity ratio, I_D/I_G, presented in Fig. 11(b), gradually increases from 0.79 of the pristine GO to close to 1.0 in the first 120 pulses, where it tends to saturate. Such behavior complies with the saturation effect observed in the respective *I–V* characteristics. Such similarity in the evolution of I_D/I_G and mobility with N shown in Figs. 11(b) and 10(b) provides important information on the GO lattice structure attained following at various levels of reduction.

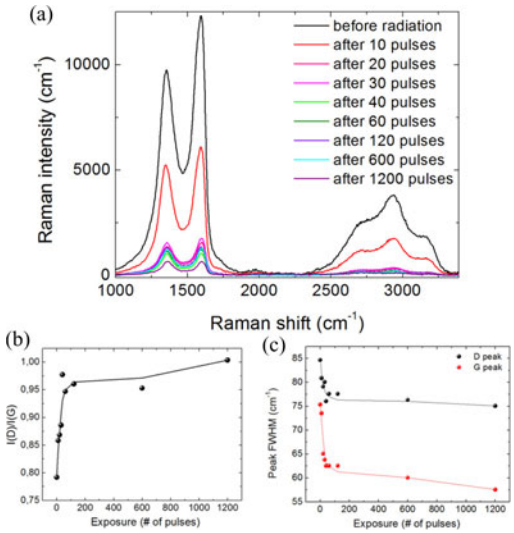

Fig. 11. (a) Micro-Raman measurements performed at the same spot onto the GO area before (pristine) and after irradiation with different N states; (b) dependence of the I_D/I_G ratio on the number of the laser pulses; (c) dependence of the D and G peaks FWHM on the number of the laser pulses. From [31].

It had been found that, an increase of I_D/I_G ratio indicates disordering of graphite but ordering of amorphous carbon structures [48]. In particular, in the case of very disordered structures, such as amorphous carbon or low mobility GO, the D band intensity is related to the density of the six-membered aromatic rings [49]. Besides this, the G band stems from in-plane bond stretching of sp^2 carbon atoms and is not necessarily related to the presence of six-membered rings. Therefore, the I_D/I_G ratio should increase with increasing ordering. Based on the analysis of Lucchese *et al.*, one can calculate, using the measured I_D/I_G values, the average distance between defects, L_D, within the GO lattice [50]. The results are presented in Fig. 11(b) and predict an increase of L_D from 10 to 11 nm after the first 120 pulses, where it saturates. This ordering effect together with the laser-induced desorption of oxygen groups contributed to the mobility rise in GO. Once the GO lattice becomes more ordered, following reduction with 120 pulses, both the I_D/I_G and the mobility tend to saturate suggesting a limit in GO lattice ordering and oxygen removal under the irradiation conditions used.

The aforementioned results indicate that upon excitation with nanosecond pulses, GO sheets absorbed the laser energy which was rapidly converted into heat and subsequent photothermal G peaks get desorption of oxygen groups, mainly of hydroxyl and epoxides, takes place [27]. With the progression of laser exposure, thermal effects become more and more pronounced [51], giving rise to photothermal breakage of carbon bonds which reestablishes the lattice defects. TA is a commonly used method for the GO reduction. It is reported that the exothermic reduction of GO occurs around 200–230 °C, attributed to the decomposition of the oxygen-containing groups present in the GO lattice. On the other hand, oxidation, and therefore, sublimation of the carbon backbone is anticipated to occur above 500 °C [52], [53]. Using a FEM to solve a simple heat balance equation for similar laser pulse and fluence to those used here, it is demonstrated that the temperature on the surface can reach over 500 °C for GO films thicker than six layers, while the temperature decreases rapidly along the depth [27]. Therefore, laser irradiation could partially ablate the topmost layers, as indicated by the lowering the Raman peaks intensities, while the lower layers were deoxygenated by photothermal reduction. As a result the GO sheets left on the sample exhibit improved conductivity. Besides this, the prediction that the GO temperature can reach 500 °C complies with the observation that the conductivity improvement due to laser photothermal effect is higher compared to that of TA at 200 °C. Finally, it should be noted that the transistor characteristics obtained due to the laser treatment remained stable even after TA in nitrogen for 1 h at 200 °C. This indicates that the laser reduction process brought about permanent changes in the electronic behavior of the GO FETs.

Another reduction mechanism that may be considered here is the photochemical desorption of oxygen groups. It is proposed that photochemical reduction of GO can be facilitated by the presence of the adsorbed water [34]. In particular, the energy from recombination of photoexcited carriers is used for water dissociation into molecular oxygen and hydrogen ions (protons). Protons are inherently strong reducing agents giving rise to removal of oxygen functional groups from GO lattice to form r-GO. Laser reduction experiments are currently in progress to elucidate the contribution of each of the candidate mechanisms.

IV. Conclusion

In conclusion, we demonstrated an efficient laser-based method for the *in-situ* reduction of transparent GO nanolayers that were solution-processed onto temperature sensitive substrates such as plastic. The method is particularly attractive considering that it is applied *in situ*, in one-step, and does not require additional transfer of the reduced GO film to the substrate. Compared to chemical and high temperature thermal annealing methods, pulsed laser photoreduction is simple, very fast, energy efficient, and poisonous material free. Preliminary work shows that the resulting laser-reduced GO films can be effectively integrated in flexible OPV cells, as the transparent electrode, replacing ITO as well as for the fabrication of FETs with promising performance characteristics.

Furthermore, by employing the optical schemes and of-the-shelve translation systems developed for industrial lasers, rapid and large-area processing can be realized, hence, making this technique easily adaptable to flexible roll-to-roll mass manufacturing. In this way, the proposed *in-situ* laser assisted reduction of graphene flexible films can be utilized as a component on self-powered and wearable electronic devices, including plastic solar cells, LEDs, batteries, sensors, e-papers, and implantable biomedical devices.

References

[1] J. H. Burroughes, D. D. C. Bradley, A. R. R. Brown, N. Marks, K. Mackay, R. H. Friend, P. L. Burn, and A. B. Holmes, "Light-emitting diodes based on conjugated polymers," *Nature*, vol. 347, pp. 539–541, 1990.

[2] A. Facchetti, "Semiconductors for organic transistors," *Mater. Today*, vol. 10, pp. 28–37, 2007.

[3] C. J. Brabec, "Organic photovoltaics: Technology and market," *Solar Energy Mater. Solar Cell*, vol. 83, pp. 273–292, 2004.

[4] T. W. Kelley, P. F. Baude, C. Gerlach, D. E. Ender, D. Muyres, M. A. Haase, D. E. Vogel, and S. D. Theiss, "Recent progress in organic electronics: Materials, devices and processes," *Chem. Mater.*, vol. 16, pp. 4413–4422, 2004.

[5] K. Jain, M. Klosner, and M. Zemel, "Flexible electronics and displays: High resolution, roll to roll, projection lithography and photoablation processing technologies for high-throughput production," *Proc. IEEE*, vol. 93, no. 8, pp. 1500–1510, Aug. 2005.

[6] W. J. Yu, S. H. Chae, and S. Y. H. Lee, "Small hysteresis nanocarbon-based integrated circuits on flexible and transparent plastic substrate," *Nano Lett.*, vol. 11, pp. 1344–1350, 2011.

[7] R. Baughman, A. A. Zakhidov, and W. A. de Heer, "Carbon nanotubes—The route toward applications," *Science*, vol. 297, pp. 787–792, 2002.

[8] J.-Y. Lee, S. T. Connor, Y. Cui, and P. Peumans, "Solution-processed metal nanowire mesh transparent electrodes," *Nano Lett.*, vol. 8, pp. 689–692, 2008.

[9] G. Shen, P.-C. Chen, K. Ryu, and C. Zhou, "Devices and chemical applications sensors of metal oxide nanowires," *J. Mater. Chem.*, vol. 19, pp. 828–839, 2009.

[10] A. K. Geim and K. S. Novoselov, "The rise of graphene," *Nat. Mater.*, vol. 6, pp. 183–191, 2007.

[11] A. H. C. Neto, F. Guinea, N. M. R. Peres, K. S. Novoselov, and A. K. Geim, "The electronic properties of graphene," *Rev. Mod. Phys.*, vol. 81, pp. 109–162, 2009.

[12] G. Eda, G. Fanchini, and M. Chhowalla, "Large-area ultrathin films of reduced graphene oxide as a transparent and flexible electronic material," *Nature Nanotechnol.*, vol. 3, pp. 270–274, 2008.

[13] F. Schwierz, "Graphene Transistors," *Nature Nanotechnol.*, vol. 5, pp. 487–496, 2010.

[14] E. Stratakis, G. Eda, H. Yamaguchi, E. Kymakis, C. Fotakis, and M. Chhowalla, "Free-standing graphene on microstructured silicon vertices for enhanced field emission properties," *Nanoscale*, vol. 4, pp. 3069–3074, 2012.

[15] M. M. Stylianakis, G. D. Spyropoulos, E. Stratakis, and E. Kymakis, "Solution-processable graphene linked to 3,5-dinitrobenzoyl as an electron acceptor in organic bulk heterojunction photovoltaic devices," *Carbon*, vol. 50, pp. 5554–5561, 2012.

[16] E. Stratakis, M. Stylianakis, E. Koudoumas, and E. Kymakis, "Plasmonic organic photovoltaic devices with graphene based buffer layers for stability and efficiency enhancement," *Nanoscale*, vol. 5, pp. 4144–4150, 2013.

[17] K. S. Novoselov, D. Jiang, F. Schedin, T. J. Booth, V. V. Khotkevich, S. V. Morozov, and A. K. Geim, "Two-dimensional atomic crystals," *Proc. Natl. Acad. Sci. USA*, vol. 102, pp. 10451–15453, 2005.

[18] M. J. Allen, V. C. Tung, and R. B. Kaner, "Honeycomb carbon: A review of graphene," *Chem. Rev.*, vol. 110, pp. 132–145, 2010.

[19] K. S. Kim, Y. Zhao, H. Jang, S. Y. Lee, J. Kim, K. S. Kim, J. H. Ahn, P. Kim, J. Y Choi, and B. H. Hong, *Nature*, vol. 457, pp. 706–710, 2009.

[20] A. Dato, V. Radmilovic, Z. Lee, J. Phillips, and M. Frenklach, "Substrate–free gas phase synthesis of graphene sheet," *Nano Lett*, vol. 8, pp. 2012–2016, 2008.

[21] C. Soldano, A. Mahmood, and E. Dujardin, "Production, properties and potential of graphene," *Carbon*, vol. 48, pp. 2127–2150, 2010.

[22] C. Mattevi, G. Eda, S. Agnoli, S. Miller, K. A. Mkhoyan, O. Celik, D. Mastrogiovanni, G. Granozzi, E. Garfunkel, and M. Chhowalla, "Evolution of electrical, chemical, and structural properties of transparent and conducting chemically derived graphene thin films," *Adv. Funct. Mater.*, vol. 19, pp. 2577–2583, 2009.

[23] S. Stankovich, D. A. Dikin, R. D. Piner, K. A. Kohlhaas, A. Kleinhammes, Y. Jia, Y. Wu, S. T. Nguyen, and R. S. Ruoff, "Synthesis of graphene based nanosheets via chemical reduction of exfoliated graphite oxide," *Carbon*, vol. 45, pp. 1558–1565, 2007.

[24] Z. Y. Yin, S. Y. Sun, T. Salim, S. X. Wu, X. Huang, Q. Y. He, Y. M. Lam, and H. Zhang, "Organic photovoltaic devices using highly flexible reduced graphene oxide films as transparent electrodes," *ACS Nano*, vol. 4, pp. 5263–5268, 2010.

[25] P. H. Wöbkenberg, G. Eda, D.-S. Leem, J. C. de Mello, D. D. C. Bradley, M. Chhowalla, and T. D. Anthopoulos, "Reduced graphene oxide electrodes for large area organic electronics," *Adv. Mater.*, vol. 23, pp. 1558–1562, 2011.

[26] G. Williams, B. Seger, and P. V. Kamat, "The prospective two-dimensional graphene nanosheets: Preparation, functionalization and applications," *ACS Nano*, vol. 2, pp. 1487–1491, 2008.

[27] L. J. Cote, R. C. Silva, and J. X. Huang, "Flash reduction and patterning of graphite oxide and its polymer composite," *J. Amer. Chem. Soc.*, vol. 131, pp. 11027–11032, 2009.

[28] Y. L. Zhang, Q. D. Chen, H. Xia, and H. B. Sun, "Designable 3D nanofabrication by femtosecond laser direct writing," *Nano Today*, vol. 5, pp. 435–448, 2010.

[29] S. H. Ko, H. L. Pan, C. P. Grigoropoulos, C. K. Luscombe, J. M. J. Frechet, and D. Poulikakos, "All-injet printed flexible electronics fabrication on a polymer substrate by low temperature high resolution selective laser sintering of metal nanoparticles," *Nanotechnology*, vol. 18, pp. 1–8, 2007.

[30] E. Kymakis, K. Savva, M. M. Stylianakis, C. Fotakis, and E. Stratakis, "Flexible organic photovoltaic cells with in-situ non-thermal photoreduction of spin coated graphene oxide," *Adv. Funct. Mater.*, vol. 23, pp. 2742–2749, Jun. 2013.

[31] C. Petridis, Y.-H. Lin, K. Savva, G. Eda, E. Kymakis, T. D. Anthopoulos, and E. Stratakis, "Post-fabrication, in-situ laser reduction of graphene oxide devices," *Appl. Phys. Lett.*, vol. 102, pp. 093115-1–093115-5, 2013.

[32] Z. Luo, Y. Lu, L. A. Somers, and A. T. C Johnson, "High yield preparation of macroscopic graphene oxide membranes," *J. Amer. Chem. Soc.*, vol. 131, pp. 898–899, 2009.

[33] S. De and J. N. Coleman, "Are there fundamental limitations on the sheet resistance and transmittance of thin graphene Films," *ACS Nano*, vol. 4, pp. 2713–2720, 2010.

[34] K. S. Subrahmanyam, P. Kumar, A. Nag, and C. N. Rao, "Blue light emitting graphene based materials and their use in generating white light," *Solid-State Commun.*, vol. 150, pp. 1774–1777, 2010.

[35] V. Abdelsayed, S. Moussa, H. M. Hassan, H. S. Aluri, M. M. Collinson, and M. Samy El-Shall, "Photothermal deoxygenation of graphite oxide with laser excitation in solution and graphene-aided increase in water temperature," *J. Phys. Chem. Lett.*, vol. 1, pp. 2804–2810, 2010.

[36] Z. H. Liu, Z. M. Wang, X. Yang, and K. Ooi, "Intercalation of organic ammonium ions into layered graphite oxide," *Langmuir*, vol. 18, pp. 4926–4932, 2002.

[37] B. N. Chichkov, C. Momma, S. Nolte, F. von Alvensleben, and A. Tunnermann, "Femtosecond, picosecond and nanosecond laser ablation of solids," *Appl. Phys. A.*, vol. 63, pp. 109–115, 1996.

[38] H. D. Wang, W.-G. Ma, X. Zhang, W. Wang, and Z. Y. Guo, "Theoretical and Experimental study on the heat transport in metallic nanofilms heated by ultra short pulsed laser," *Int. J. Heat Mass Transfer*, vol. 54, pp. 967–974, 2011.

[39] S. S. Li, K. H. Tu, C. C. Lin, C. W. Chen, and M. Chhowalla, "Solution processable graphene oxide as an efficient hole transport layer in polymer solar cells," *ACS Nano*, vol. 4, no. 6, pp. 3169–3174, 2010.

[40] F. Gune, H. J. Shin, C. Biswas, G. H. Han, E. S. Kim, S. J. Chae, J. Y. Choi, and Y. H. Lee, "Layer by layer doping of few layer graphene film," *ACS Nano*, vol. 4, pp. 4595–4600, 2010.

[41] C. Biswas and Y. H. Lee, "Graphene versus carbon nanotubes in electronic devices," *Adv. Funct. Mater.*, vol. 21, pp. 3806–3826, 2011.

[42] V. C. Tung, L. M. Chen, M. J. Allen, J. K. Wassei, K. Nelson, R. B. Kaner, and Y. Yang, "Low-Temperature solution processing of graphene-carbon nanotube hybrid materials for high-performance transparent conductors," *Nano Lett.*, vol. 9, no. 5, pp. 1949–1955, 2009.

[43] H. Zang and Y. Miyamoto, "Graphene production by laser on graphene oxide: An ab initio prediction," *Phys. Rev. B, Condens. Matter*, vol. 85, pp. 033402-1–033402-4, 2012.

[44] Y. Zhou, Q. L. Bao, B. Varghese, L. A. L. Tang, C. K. Tan, C. H. Sow, and K. P. Loh, "Microstructuring of graphene oxide nanosheets using direct laser writing," *Adv. Mater.*, vol. 22, pp. 67–71, 2010.

[45] S. A. Wang, P. K. Ang, Z. Q. Wang, A. L. L. Tang, J. T. L. Thong, and K. P. Loh, "High mobility, printable, and solution-processed graphene electronics," *Nano Lett.*, vol. 10, pp. 92–98, 2010.

[46] F. Tuinstra and J. L. Koenig, "Raman spectrum of graphite," *J. Chem. Phys.*, vol. 53, pp. 1126-1–1126-5, 1970.

[47] K. N. Kudin, B. Ozbas, H. C. Schniepp, R. K. Prud'homme, I. A. Aksay, and R. Car, "Raman spectra of graphite oxide and functionalized graphene sheets," *Nano Lett.*, vol. 8, pp. 36–41, 2008.

[48] A. C. Ferrari and J. Robertson, "Interpretation of Raman spectra of disordered and amorphous carbon," *Phys. Rev. B, Condens. Matter*, vol. 61, pp. 14095–14107, 2000.

[49] C.-Y. Su, Y. Xu, W. Zhang, J. Zhao, A. Liu, X. Tang, C.-H. Tsai, Y. Huang, and L.-J. Li, "Highly efficient restoration of graphitic structure in graphene oxide using alcohol vapors," *ACS Nano*, vol. 4, no. 9, pp. 5285–5292, 2010.

[50] M. M. Lucchese, F. Stavale, E. H. Martins Ferreira, C. Vilani, M. V. O. Moutinho, R. B. Capaz, C. A. Achete, and A. Jorio, "Quantifying ion-induced defects and Raman relaxation length in graphene," *Carbon*, vol. 48, pp. 1592–1597, 2010.
[51] B. N. Chichkov, C. Momma, S. Nolte, F. von Alvensleben, and A. Tünnermann, "Femtosecond, picosecond and nanosecond laser ablation of solids," *Appl. Phys. A.*, vol. 63, pp. 109–115, 1996.
[52] H. K. Jeong, Y. P. Lee, M. H. Jin, E. S. Kim, J. J. Bae, and Y. H. Lee, "Thermal stability of graphene oxide," *Chem. Phys. Lett.*, vol. 470, pp. 255–258, 2009.
[53] R. Bissessur, P. K. Y. Liu, W. White, and S. F. Scully, "Encapsulation of polyanillines into graphite oxide," *Langmuir*, vol. 22, pp. 1729–1734, 2006.

Emmanuel Kymakis (M'05) was born in Heraklion, Greece, in 1977. He received the B.Eng. (First class) degree in electrical engineering and electronics from Liverpool University, Liverpool, U.K., in 1999 and the Ph.D. degree in electrical engineering from Cambridge University, Cambridge, U.K., in 2003. He and Prof. Amaratunga are the inventors of the polymer-nanotube solar cell. He is currently an Associate Professor of Electronic Materials and Devices at the Electrical Engineering Department, Technological Educational Institute (TEI) of Crete, Heraklion, Greece. He also heads the Nanomaterials & Organic Electronics group of the Center of Materials Technology and Photonics. Before joining TEI of Crete, he worked as a Technical Consultant offering engineering and consultancy services in the field of photovoltaic and solar thermal power plants for various Greek and international investors and private companies. He has more than 40 publications with more than 2000 citations. His research interests include the areas of novel materials and nanostructured composites and their incorporation in optoelectronic devices, such as photovoltaic devices and field emission displays. Furthermore, his recent research efforts are concentrated in the investigation of carbon nanotubes and graphene, and their unique interactions with polymers for energy conversion systems. He has been selected as an Honorary Lecturer in the UConn, and received an Isaac Newton and an EPSRC studentship. He is the Greek National Representative in two COST actions. He is also a member of the Graphene Flagship Consortium. Prof. Kymakis is a Member of the Institution of Engineering and Technology and the Technical Chamber of Greece.

Constantinos Petridis was born in Athens, Greece, in 1972. He received the B.S. degree in physics from the University of Crete, Heraklion, Greece, in 1995, and the M.Sc. degree in optoelectronics, lasers and applications in 1996 and the Ph.D. degree in nonlinear optics in 2001 both from the University of St-Andrews, St Andrews, U.K. From 2003 to 2004, he was a Research Assistant with NonLinear Optics Group, ICFO, Spain. From 2004 to 2009, he was a contract Assistant Professor in the Department of Electronics, TEI of Crete, Heraklion, Greece, where Since 2009, he has been a Lecturer and the project manager of the LLP Erasmus Programme:Multilateral Projects, entitled "Organic Electronics and Applications" (2013–2015). He is a Member of the Nanomaterials & Organic Electronics group, the Center of Materials Technology and Photonics, TEI of Crete.

Thomas D. Anthopoulos was born in Kastoria, Greece, in 1975. He received the B.Eng. and Ph.D. degrees, from Staffordshire University, Staffordshire, U.K. He then moved to University of St. Andrews, St Andrews, U.K., where he worked as a Postdoctoral Researcher on organic light-emitting diodes. In 2003, he joined Philips Research Laboratories, The Netherlands to work on organic semiconductors for optoelectronic applications. In 2005, he was received an EPSRC Advanced Fellowship and in 2007, a RCUK Fellowship both hosted in the Department of Physics, Imperial College London, London, U.K., where is currently a Professor of experimental physics in the same department and The Centre for Plastic Electronics. His current research interests include nanopatterning, the physics of carbon-based, metal oxides and hybrid semiconductors, and large-volume optoelectronics. Prof. Anthopoulos received a European Research Council (ERC) Starting Grant Award, the Ben Sturgeon Prize 2011 awarded by the Society for Information Display (SID – U.K. and Ireland), the The Alfred Woodhead Best Paper Award (SID 2007), and a Research Excellence Award from Imperial College London.

Emmanuel Stratakis received the Ph.D. degree in 2001 from the University of Crete, Heraklion, Greece. He is currently a Researcher at the Institute of the Electronic Structure and Laser (IESL) of the Foundation for Research and Technology-Hellas (FORTH) and an Adjunct Professor at the Department of Materials Science and Technology, University of Crete. After graduating, he joined as a Visiting Researcher the IESL-FORTH working on the ultrafast laser engineering of materials and as an Adjunct Professor at the Department of Materials Science and Technology, University of Crete, where he remains until today. In the fall semesters of 2006 and 2008, he was a Visiting Researcher at the Department of Mechanical Engineering, University of California, Berkeley, USA. In 2007, he was an elected Researcher at IESL-FORTH where he is leading the "Ultrafast Laser Micro- and Nano- processing" activity. His research group has extensive experience on the development of novel ultrafast laser-based techniques for (a) direct micro- and nanoprocessing of materials, (b) laser nanomaterials synthesis, modification and functionalization for organic electronics, and (c) the fabrication of dual rough biomaterials surfaces for biomedical applications. Dr Stratakis has published seven chapters in scientific books, 65 papers in refereed journals, and has received 850 total citations. His h-index is 19. Dr. Stratakis is a Member of the European Physical Society.